10-1-1995

Imaging and Spectroscopy of Damped Lyα Quasi-Stellar Object Absorption-Line Clouds

James Lowenthal
University of California, Santa Cruz, jlowenth@smith.edu

Craig J. Hogan
University of Washington

Richard F. Green
National Optical Astronomy Observatory

Bruce Woodgate
Kitt Peak National Observatory

Adeline Caulet
Kitt Peak National Observatory

See next page for additional authors

Recommended Citation

Authors

James Lowenthal, Craig J. Hogan, Richard F. Green, Bruce Woodgate, Adeline Caulet, Larry Brown, and Jill Bechtold

IMAGING AND SPECTROSCOPY OF DAMPED Lyα QUASI-STELLAR OBJECT ABSORPTION-LINE CLOUDS[1]

JAMES D. LOWENTHAL,[2,3,4] CRAIG J. HOGAN,[5] RICHARD F. GREEN,[6] BRUCE WOODGATE,[3,7]
ADELINE CAULET,[3,8] LARRY BROWN,[3,7] AND JILL BECHTOLD[9]

ABSTRACT

We present the results of a multifaceted search for line emission from the vicinities of high-redshift quasi-stellar object (QSO) absorption-line clouds, most of them damped Lyα systems at $z \gtrsim 2$. Seven fields containing QSOs with known intervening damped Lyα absorbers were imaged with the GSFC Fabry-Perot Imager to search for diffuse redshifted Lyα. Apart from the one Lyα companion galaxy reported previously, no confirmed extended Lyα emission was detected down to 3 σ flux levels of around 3×10^{-17} ergs s^{-1} cm^{-2}, corresponding to star formation rates $\lesssim 1$ $M_{\odot}$ yr^{-1}, assuming case B recombination, a reasonable initial mass function, and negligible extinction by dust.

One of the damped Lyα systems studied here, toward Q0836+113, has been reported to show faint, extended Lyα emission. While our Lyα images of that field are not sensitive enough to confirm the reported flux levels, we did detect and spectroscopically confirm redshifted [O II] $\lambda 3727$ and continuum emission from a closer intervening system, a Mg II system at $z = 0.788$, at the same spatial position as the reported Lyα emission from the more distant object, and we suggest the possibility that all the observations of this field can be explained by the closer system alone.

Six damped Lyα systems, including two that were imaged with the Fabry-Perot, were also imaged with two-dimensional long-slit CCD spectroscopy at ~ 2 Å resolution in the core of the Lyα absorption line. No convincing Lyα emission was found from any of the systems, including Q0836+113, for which our sensitivity was again insufficient to confirm the previously reported extended Lyα emission. However, there is yet another independent claim of Lyα emission from that cloud, but spatially unresolved, in conflict with the report of extended emission; our observations do not reproduce the report of compact Lyα emission, which should have appeared at about the 7 σ level.

Although observationally allowable quantities of dust in the damped Lyα clouds can in some cases quench Lyα flux by up to several orders of magnitude, several of the damped clouds studied here are arguably metal and dust poor, leading us to believe that our limits on Lyα emission generally constrain the star formation rates to be $\lesssim 10$ $M_{\odot}$ yr^{-1}, comparable to normal Sc galaxies today. Whatever their exact nature, the damped Lyα clouds therefore appear not to be spectacular primeval galaxies seen in the act of forming a galaxy's worth of stars.

Subject heading: quasars: absorption lines

1. INTRODUCTION

Studying quasi-stellar object (QSO) absorption-line systems at high redshift reveals important information about the early universe that cannot be gathered any other way. It is by now quite secure that metal-line clouds such as Mg II and C IV systems are directly associated with some form of galaxy, and indeed they are routinely imaged in continuum and line emis-sion out to redshifts beyond one (e.g., Yanny, York, & Williams 1990; Bergeron & Boissé 1991; Steidel & Dickinson 1992). Furthermore, galaxies selected by the absorption lines they imprint on the spectra of distant QSOs are for the most part much higher redshift objects than the bulk of galaxies discovered via their emission properties, for example in deep blank field galaxy surveys (e.g., Broadhurst, Ellis, & Shanks 1988; Tyson 1988; Lilly, Cowie, & Gardner 1991), which rarely produce median redshifts greater than $\frac{1}{2}$. QSOs have been observed at redshifts approaching five, and absorption-line systems are thus observable to almost the same distances. While there is continuing debate over the morphological form that metal-line QSO absorption line systems take, e.g., gas-rich dwarf galaxies versus extended disk systems versus H II regions in evolving spheroids, the chemical and kinematic properties inferred from the metal and hydrogen lines, the observed column densities, and the observed clustering characteristics are all reminiscent of sight lines through turbulent, gaseous regions of normal galaxies.

Damped Lyα clouds, so called because they have sufficient column densities of neutral hydrogen [N(H) $\gtrsim 2 \times 10^{20}$ cm^{-2}] that their Lyα absorption lines saturate in the core and show broad damping wings, occupy the high end of the column

---

[2] UCO/Lick Observatory, University of California, Santa Cruz, CA 95064; james@lick.ucsc.edu.

[3] Visiting astronomer, Kitt Peak National Observatory and Cerro Tololo Inter-American Observatory.

[4] Hubble Fellow.

[5] University of Washington, Astronomy Department, FM-20, Seattle, WA 98195.

[6] National Optical Astronomical Observatory, P.O. 26732, Tucson, AZ 85732.

[7] Goddard Space Flight Center, Code 681, Greenbelt, MD 20771.

[8] Space Telescope European Coordinating Facility/ESO, Karl-Schwarzschild-Strasse 2, D-8064 Garching bei München, Germany.

[9] Steward Observatory, University of Arizona, Tucson, AZ 85721.

density distribution of all QSO absorption-line systems. Wolfe et al. (1986; the first major survey, which discovered 15 confirmed damped systems) and Lanzetta et al. (1991; 22 more confirmed systems; see also Lu & Wolfe 1994) have argued on the basis of the observed statistics that the damped clouds are the dominant form of neutral hydrogen at $z \sim 2.5$, containing a total H I mass comparable to that in stars in disk galaxies today, which in turn has prompted their identification as the progenitors of present-day disk galaxies; this suggestion is supported by the narrow velocity width but broad spatial extent ($> 8 \, h_{100}$ kpc) observed in the H I 21 cm absorption line of at least one damped cloud (Q0458−020; Briggs et al. 1989). All damped Lyα systems are associated with Mg II absorption and frequently show C IV lines as well as other low- and high-ionization species.

If indeed the damped Lyα clouds are young galaxies, we might expect them to be experiencing luminous bursts of massive star formation, which in turn would produce the ionizing UV radiation necessary for Lyα and other nebular emission lines. Such emission, if detectable, could provide a wealth of direct information about the spatial extents, masses, distributions, morphologies, metallicities, and star formation histories of the damped clouds in particular and, perhaps, high-redshift galaxies in general. This would be particularly valuable in a sample not *selected* on the basis of emission properties, but by its absorption. Since absorbers are everywhere and their statistical properties are well studied, even a tiny sample of associated emission can sharpen our picture of global conditions at high redshift.

Motivated by this possibility, several groups have searched the damped clouds in the optical for redshifted Lyα emission, and in the near-IR for redshifted [O II] $\lambda 3727$, [O III] $\lambda 5007$, and Hβ emission. These searches represent a more directed approach to the problem of identifying young galaxies at high redshift than "blank sky" and field galaxy surveys, which examine regions of the sky independent of prior knowledge of damped Lyα or other QSO absorption-line systems. In the near-IR, Elston et al. (1991) reported Hβ and [O II] $\lambda 3727$ emission from the damped cloud at $z = 1.998$ toward Q1215+333 at levels implying star formation rates comparable to those in active starburst galaxies today; however, subsequent observations have not confirmed that detection, and so we regard it here as suspect (see also Caulet & McCaughrean 1992 and Hu et al. 1993 for additional studies in the near-IR). Furthermore, inspired by the spectral detection of molecular CO emission from the *IRAS* galaxy FSC 10214+4715 at $z = 2.286$ (Brown & Vanden Bout 1991; Solomon, Radford, & Downes 1992), Brown & Vanden Bout (1993) reported the detection of CO emission from the damped Lyα cloud at $z = 2.14$ toward Q0528−250 and inferred a molecular gas mass of $7 \times 10^{11} \, M_{\odot}$, comparable to the total mass of a large spiral galaxy today. However, a more recent and sensitive search by Wiklind & Combes (1994) was unable either to confirm the emission from the Q0528−250 cloud or to detect emission from any of seven other damped Lyα clouds ranging in redshift from 0.5 to 2.8. A similar search for H I 21 cm emission from the damped Lyα cloud at $z = 3.390$ toward Q0000−2619 (Taramopoulos, Briggs, & Trunshek 1994) resulted only in an upper limit on the cloud's neutral hydrogen mass of $1.5–5 \times 10^{13} \, M_{\odot}$. In a related study, Uson, Bagri, & Cornwell (1991) reported the discovery of H I 21 cm emission from a putative Zeldovich pancake at $z = 3.4$—not technically a QSO absorption-line cloud—but independent radio observations (Briggs 1993) and a search for Lyα emission (Rhee, Loken, & Febre 1993) from the same region have both produced negative results.

While the near-IR and radio produce tantalizing hints of detections, directed searches for Lyα emission from radio-quiet high-redshift galaxies have been almost uniformly unsuccessful, with some notable exceptions. Many hours of integration time using CCDs on large telescopes with long-slit spectroscopy (Foltz, Chaffee, & Weymann 1986) and narrowband imaging (Smith et al. 1989; Deharveng, Buat, & Bowyer 1990) produced upper limits well below the levels of Lyα emission expected for disk galaxies supporting star formation at rates similar to those observed today. When Hunstead, Pettini, & Fletcher (1990, hereafter HPF) reported the detection of a narrow, spatially unresolved spike of Lyα emission in the bottom of the damped Lyα absorption line in the spectrum of Q0836+113, it seemed that at last the Rosetta stone of observational cosmology, a primeval galaxy, had been found, and that at least one damped cloud could plausibly be a gas-rich dwarf galaxy and not an extended disk. However, Wolfe et al. (1992) were unable to confirm the unresolved emission with a deep spectrum taken at the Palomar 5 m telescope; rather, they reported faint *extended* emission observed with a narrow-band filter centered on redshifted Lyα for the damped cloud, at a level much lower than the HPF result, supporting the hypothesis that the clouds are large by galactic scales, $r \gg 10$ kpc. The results reported here cast doubt on both sets of results.

Finally, in a separate paper (Lowenthal et al. 1991), we reported the discovery of a luminous Lyα companion galaxy to the damped cloud at $z = 2.3$ toward PHL 957. Separated from the QSO line of sight by 48″ (some $200 \, h_{100}^{-1}$ kpc at $z = 2.3$, for $q_0 = 0.5$), the galaxy shows strong Lyα, C IV $\lambda 1548$, and He II $\lambda 1640$ emission lines, so in this case at least there is little doubt about the reality of the high-redshift identification. The object also displays continuum corresponding to a current galaxy with $L = 5L_*$, but no detectable X-ray or radio emission. What appeared to be a similar object associated with the $z = 3.4$ cloud toward Q0000−2619 was detected by Turnshek et al. (1991). However, more recent observations by Machetto et al. (1993) both showed that the source is an [O II] $\lambda 3727$–emitting galaxy at $z = 0.4$ and revealed a more convincing companion galaxy candidate in the same field, an identification strengthened by broadband data presented by Steidel & Hamilton (1992). Also using narrow-band imaging, Moller & Warren (1993) detected three emission-line sources near the damped Lyα cloud at $z = 2.81$ toward Q0528−250 (the same line of sight from which Brown & Vanden Bout 1993 reported CO emission from a lower redshift cloud). The damped cloud is unique in that it lies at the same redshift as the background QSO, suggesting that the Lyα emission may be associated directly in some way with the QSO itself.

Taken together with extensive searches conducted for Lyα-emitting galaxies in "blank sky" (e.g., Pritchett & Hartwick 1990; Lowenthal et al. 1990; Cowie 1988; Thompson, Djorgovski, & Trauger 1993), which have yielded uniformly null results, these detections of emission-line galaxies near damped Lyα clouds hinted at clustering of galaxies at high redshift. This possibility motivated Lowenthal (1991) and Wolfe (1993) to calculate the galaxy two-point correlation function at $z = 2.6$ and to conclude that indeed clustering had been detected at a statistically significant level. Additional evidence supporting this picture was presented by Giavalisco, Steidel, & Szalay (1994), who used strategically chosen broadband optical filters

to identify several galaxies near the Q0000−2619 Lyα emitter that had colors matching those expected for sources at $z = 3.4$. Even more direct support for clustering of damped Lyα clouds—with each other and with other galaxies—comes in the form of at least two Lyα-emitting galaxies and a cluster of IR-bright sources, all apparently associated with a cluster of damped Lyα clouds toward two close QSO lines of sight (Francis et al. 1995).

In this paper, we present the results of a multifaceted attempt to detect Lyα emission associated with 11 damped Lyα systems at $1.9 < z < 3.2$. We were primarily interested in studying the absorbing clouds themselves, including their star-forming characteristics and spatial extents, but we were keen to understand the nature of any additional companion galaxies as well.

2. OBSERVATIONS

Two search techniques lend themselves to the detection of faint line emission: long-slit spectroscopy and narrow-band imaging. Both methods operate by spreading out or rejecting the night-sky background emission, thus decreasing background noise and increasing the contrast of any line emission. The highest contrast is achieved when the spectral resolution closely matches the width of the emission line; for normal galaxies, we expect this to be in the range 100–1000 km s^{-1}.

Although the volumes sampled by the two techniques are usually comparable, corresponding to ~ 10 Mpc^3 in comoving coordinates for typical instruments at 4 m class telescopes, the shapes are quite different, with imaging searching a cube but spectroscopy searching a long flat "yardstick" that extends deep in redshift space. Furthermore, narrow-band imaging is best suited for spatially extended sources, especially if the morphology is unknown, while spectroscopy is more appropriate for detecting spatially unresolved emission coincident with the QSO line of sight; thus, the two are complementary. We have employed both methods in our survey.

2.1. Fabry-Perot Imaging

During two observing runs on 1990 January 24–26 UT and 1991 December 30–1992 January 2 UT at the Kitt Peak National Observatory (KPNO) 4 m telescope, we imaged a total of eight damped Lyα cloud fields with the Goddard Fabry-Perot Imager (GFPI). Results on one of those fields, containing the QSO PHL 957, have been published elsewhere (Lowenthal et al. 1991), and here we discuss only the remaining seven fields. The observations are summarized in Table 1.

The GFPI is essentially a tunable narrow-band filter coupled with a CCD detector and is described in detail in Caulet et al. (1992). Of the three available etalons, we used the "visible," which provides the widest transmission curve; this was to maximize our sampling of galaxies associated with but at different velocities from the absorbing clouds themselves. Generally the FWHM of the final transmission curve was about 1000 km s^{-1} for on-band exposures. During the first observing run, off-band comparison images were made by tuning the etalon to a wavelength well removed from that of the on-band, but not farther than 300 Å; the etalon gap was adjusted to transmit nearly the maximum allowable FWHM, ~ 2000 km s^{-1}, to allow shorter integration times. For off-band images during the second run, rather than using the usual 100 Å order-selecting interference filters in the optical train, we employed the KPNO "nearly Mould" broadband B filter; the etalon was left in place but tuned so that neither the emission-line wavelength of interest nor bright night-sky lines would be transmitted. This results in the transmission of several (four to six) interference orders simultaneously, again allowing shorter integration times.

The etalons are wavelength calibrated using high-pressure spectral line lamps and polynomial fits to the wavelength solutions and are controlled and held stable in wavelength via a positive capacitor/piezo-electric driver feedback loop and thermal control to 0°.5 C.

TABLE 1
SUMMARY OF FABRY-PEROT OBSERVATIONS[a]

Field	$z_{DL\alpha}$	Date (UT)	λ_{FB}[b] (Å)	$\Delta\lambda$[c] (Å)	Integration Time (s)	Number of Exposures	θ[d]
Q0045−0341......	2.810	1991 Dec 30–1992 Jan 2	4632	18	10800	4	2″.3
			B/4362	...	2250	5	2.4
Q0201+3634......	2.461	1991 Dec 30–1992 Jan 2	4206	18	10800	3	2.9
			B/4170	...	2400	4	2.7
Q0336−0142......	3.061	1991 Dec 30–1992 Jan 2	4937	20	5400	2	2.4
			B/4362	...	1350	2	2.3
Q0836+113.......	2.467	1990 Jan 24–26	4214	20	14400	4	2.3
			4023	30	7200	2	2.3
			6617	15	10800	3	2.3
			6662	15	7200	2	2.1
Q0913+0715......	2.618	1991 Dec 30–1992 Jan 2	4398	15	13500	5	2.5
			B/4362	...	2700	6	2.5
Q1209+0919......	2.581	1991 Dec 30–1992 Jan 2	4353	15	10800	4	2.3
			B/4170	...	2700	6	2.5
Q1337+113.......	2.796	1990 Jan 24–26	4614	15	20880	6	1.6
			4319	30	9000	4	2.0

[a] All data obtained at KPNO 4 m telescope.
[b] Central wavelength of Fabry-Perot etalon. "B" indicates Harris broadband B filter used instead of 100 Å order selecting filter.
[c] FWHM of Fabry-Perot transmission function.
[d] Seeing FWHM, as measured in final combined image.

We used KPNO's "Tek2" CCD, a 512 × 512 pixels device with 9 electrons pixel^{-1} readout noise. After binning by a factor of 2 in both directions, the pixel size was 0″53 on each side, giving a field of view of 2′3 × 2′3.

Images were taken of each field at the wavelength of the redshifted damped Lyα line. Additional images of the Q0836 + 113 field were taken at 6617 Å, the wavelength corresponding to redshifted C III] λ1909 from the damped Lyα system at $z = 2.467$, to explore the possibility that despite quenching of Lyα photons by dust in the absorber, a C III] line produced by massive star formation might escape relatively unhindered. For those images, off-band comparison frames were taken at 6662 Å, which was chosen to serve the double purpose of covering redshifted [O II] λ3727 from a known Mg II absorption-line system at $z = 0.788$ in the same line of sight (Turnshek et al. 1989).

Total on-band integration times range from 1.5 to 7.0 hr, divided in each case into at least two and usually four or five exposures, with the telescope shifted slightly between exposures to allow rejection of bad pixels. Integrations were sufficiently long that Poisson noise from the sky background dominated detector readout noise in each individual exposure.

The seeing during the first run ranged from 1″6 to 4″3, and during the second run it ranged from 2″3 to 2″9, as measured by the FWHM of bright stellar images in individual exposures. Because of the difficulty in combining data with significantly different seeing profiles, we rejected any images that showed a seeing FWHM greater than twice the minimum seeing FWHM obtained of that field. In practice, this meant the loss of data from only one half-night during the first run, corresponding to three on-band and two off-band images of the Q0836 + 113 field. Only the remaining data are summarized in Table 1 and discussed further below.

Several observations of spectrophotometric standard stars were taken each night at each of the program wavelengths for the purpose of converting from digital counts recorded to flux incident on the telescope. However, during the second run the weather was probably never photometric, and indeed there was occasional cirrus.

All the data reduction was carried out using the IRAF software package. The data were bias-subtracted, flat-fielded using high signal-to-noise dome flats, cosmic-ray–cleaned using a moving median box rejection algorithm, and finally shifted to fractional pixel accuracy and combined using a sigma-clipping average algorithm to make a single on-band and off-band image of each field; these are shown in Figure 1.

The multiple optical elements of the Fabry-Perot system usually produce internal ghost reflections of bright stars and galaxies. These reflections always appear in the image near the source that produced them, and always at a repeatable separation and orientation. They are therefore easily recognizable by comparison with images of bright standard stars and their ghosts' reflection patterns.

2.2. Long-Slit Spectroscopy

During three observing runs at the 4.5 m–equivalent Multiple Mirror Telescope (MMT) and one at the Steward Observatory (SO) 2.3 m telescope, we obtained long-slit CCD spectra of six damped Lyα clouds toward five high-redshift QSOs. At the MMT, a 1200 lines mm^{-1} grating was used in second order in the Red Channel CCD Spectrograph with a 1″25 × 180″ slit for a final spectral resolution of ~2 Å, while at the SO 2.3 m, an 832 lines mm^{-1} grating was used in second order in the Boller & Chivens Spectrograph with a 1″5 × 160″ slit to achieve a resolution of 1.15 Å; the pixel scale was 0″6 × 0.82 Å at the MMT and 1″6 × 0.72 Å at SO after binning the CCD by a factor of 2 spatially before readout (binning at the 2.3 m was the result of an oversight). The CCD at the 2.3 m telescope is a Texas Instruments 800 × 800 detector with 14 e^- pixel^{-1} rms read noise. Total integration times ranged from 1 hr for Q2233 + 131 to 13 hr for Q0836 + 113. Because the CCD in the MMT Red Channel could not be focused uniformly along the entire spectral range, the spectrum of Q1337 + 113 covers only the higher redshift of the two damped systems toward that QSO. These observations are summarized in Table 2.

The data were reduced as usual, including bias and flat-field corrections, two-dimensional transformation to rectilinear coordinates, and subtraction of background sky emission. The images of Q1215 + 333 displayed an anomalous wrinkled appearance reminiscent of fringing in the middle of the spectral range that we were unable to flat-field properly, reducing the sensitivity somewhat. Closeups of all six final, sky-subtracted, two-dimensional spectra in the region of the damped Lyα absorption line are shown in Figure 2, and one-dimensional extracted spectra are shown in Figure 3.

3. RESULTS

3.1. Lyα Emission from Damped Lyα Clouds

We visually inspected all the on-band Lyα Fabry-Perot images and all the spectroscopic images of the damped Lyα absorption clouds for signs of compact or extended emission. No obvious emission features were found in any of the final frames. Despite the depth and breadth of the damped Lyα

TABLE 2
SUMMARY OF SPECTROSCOPIC OBSERVATIONS

Field	$z_{DLα}$	Telescope[a]	Date (UT)	λ Range (Å)	Δλ[b] (Å)	P.A.[c]	Integration Time (s)	Number of Exposures	$θ^d$
Q0836 + 113......	2.467	MMT	1991 Jan 14–15	3870–4525	2.6	15°	46800	10	2″1
Q1215 + 333......	1.998	SO	1991 May 19	3370–3944	1.2	70	14400	4	2.9
Q1337 + 113......	2.796	MMT	1991 Jan 15	4282–4938	2.7	160	3600	3	2.6
Q1409 + 093......	2.459, 2.670	SO	1991 May 19	4066–4639	1.2	22	3600	1	2.6
Q2233 + 131......	3.150	MMT	1991 Jun 5	4747–5397	2.1	130	5400	3	1.4

[a] MMT = 4.5 m equivalent Multiple Mirror Telescope; SO = Steward Observatory 2.3 m telescope.
[b] Spectral resolution (FWHM).
[c] Position angle of slit, measured north through east.
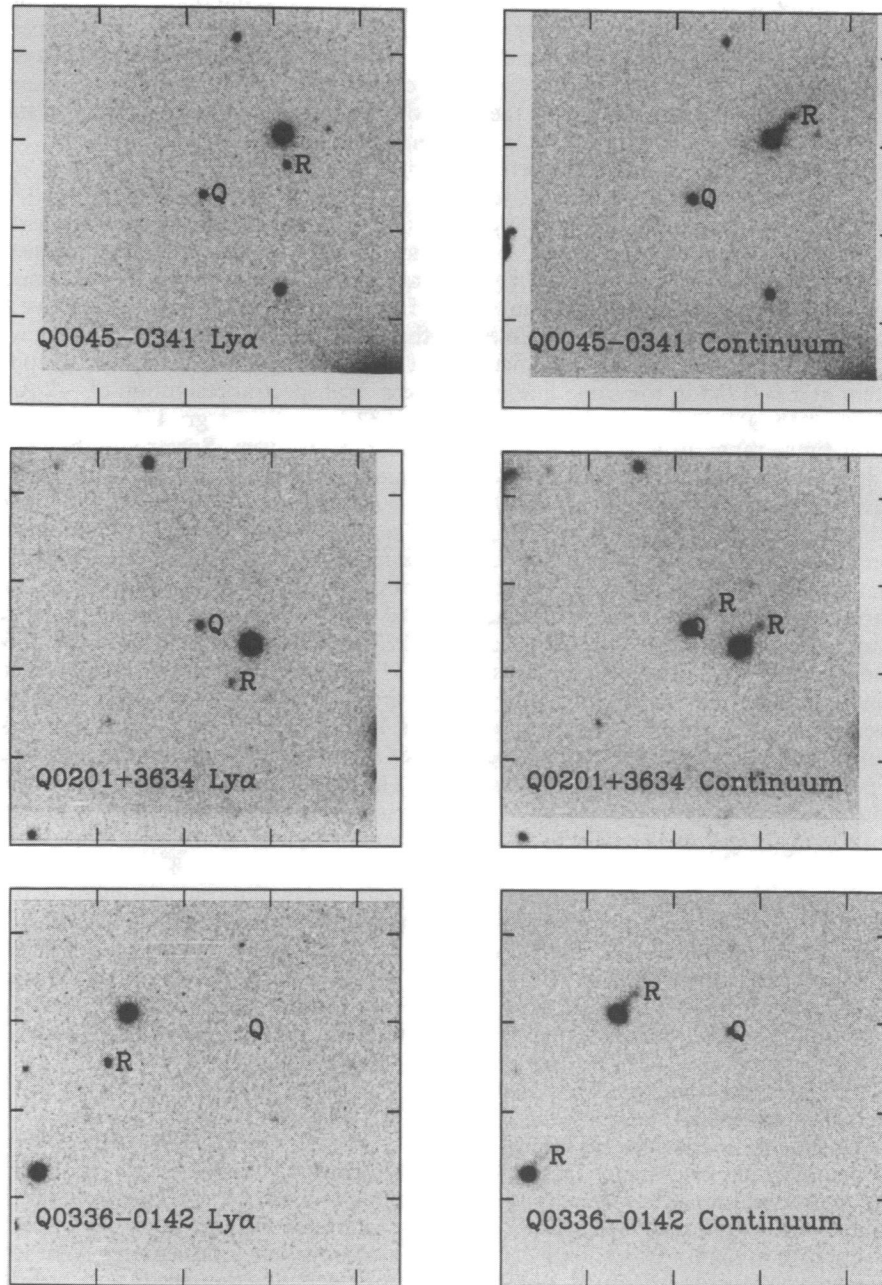[d] Seeing FWHM, as measured in final combined image.

FIG. 1.—Fabry-Perot narrow-band images of seven fields containing damped Lyα QSO absorption-line systems. In each case, the Lyα image is on the left, while the corresponding narrow- or intermediate-band continuum image is on the right. North is up and east is to the left. Tick marks are spaced at 30″ intervals. The position of each QSO is labeled "Q," and the positions of prominent internal reflection ghost images are labeled "R" immediately to the right of the artifact. Note that in the Lyα images the QSO is fainter than in the continuum images, as a result of the deep and broad damped Lyα absorption line. No Lyα emission is visible in any of the Lyα images.

absorption line, some residual flux is visible at the position of the QSO in several of the on-band Fabry-Perot frames; however, this is easily accounted for by leakage of background QSO flux into the broad wings of the FP transmission function, and in no case does it represent a convincing detection of Lyα emission spatially coincident with the QSO.

A few faint objects in both the Q0336−0142 and Q1337+113 fields appeared brighter in the on-band Fabry-Perot images than in the off-band images, but follow-up low-resolution spectroscopy at the MMT and at the Lick 3 m

telescope showed these to be objects with strong red continua (probably Galactic M-type stars) that appeared only weakly in our blue off-band frames, rather than emission-line sources. A single patch of flux is faintly visible ($\sim 2\ \sigma$) in the absorption-line trough of the damped cloud at $z = 2.459$ toward Q1409+093, but since only a single image was obtained of this object and a confirmation was impossible due to weather, we regard this as a nondetection and treat all seven Fabry-Perot and all six spectroscopic results as upper limits on Lyα emission from the damped clouds.
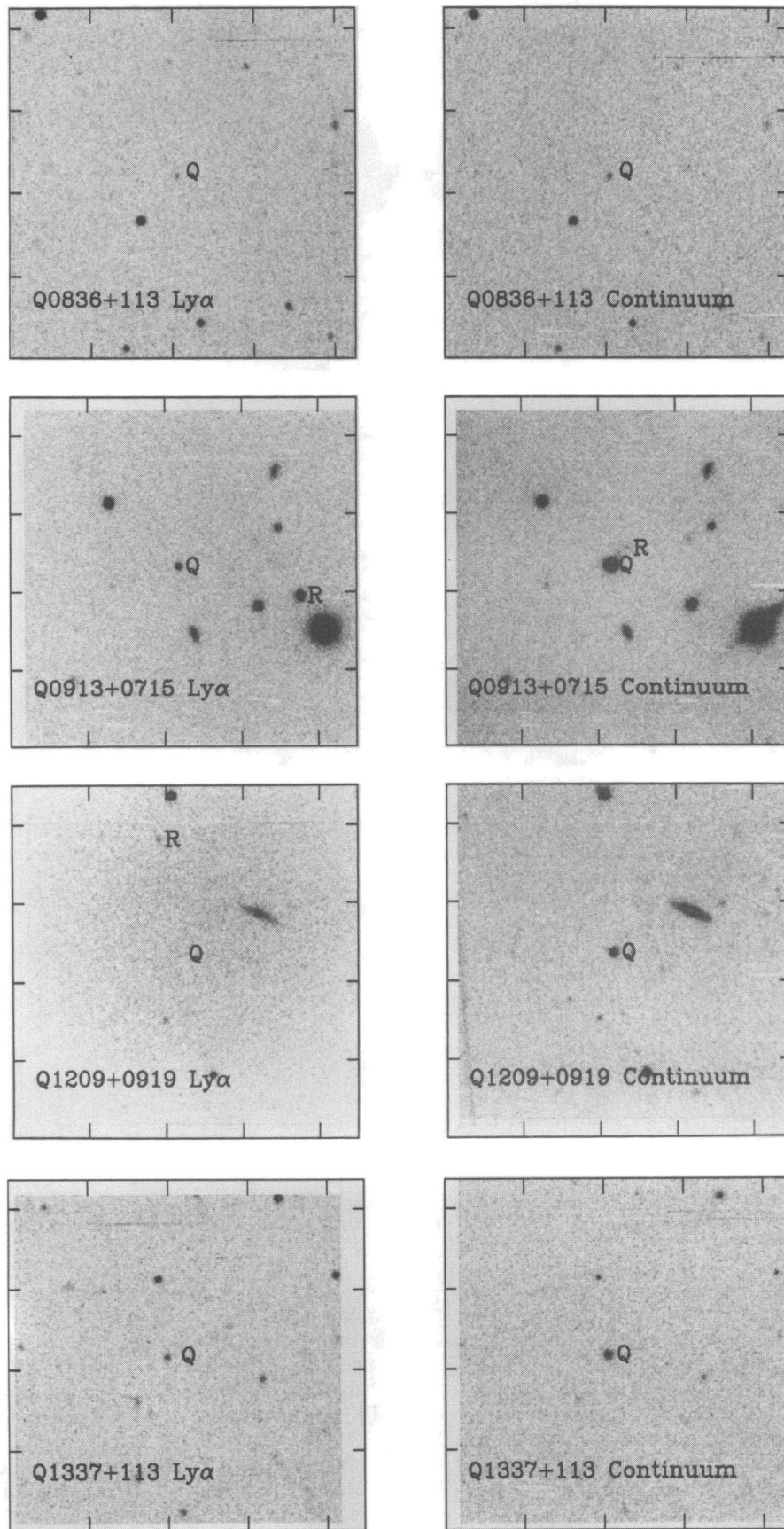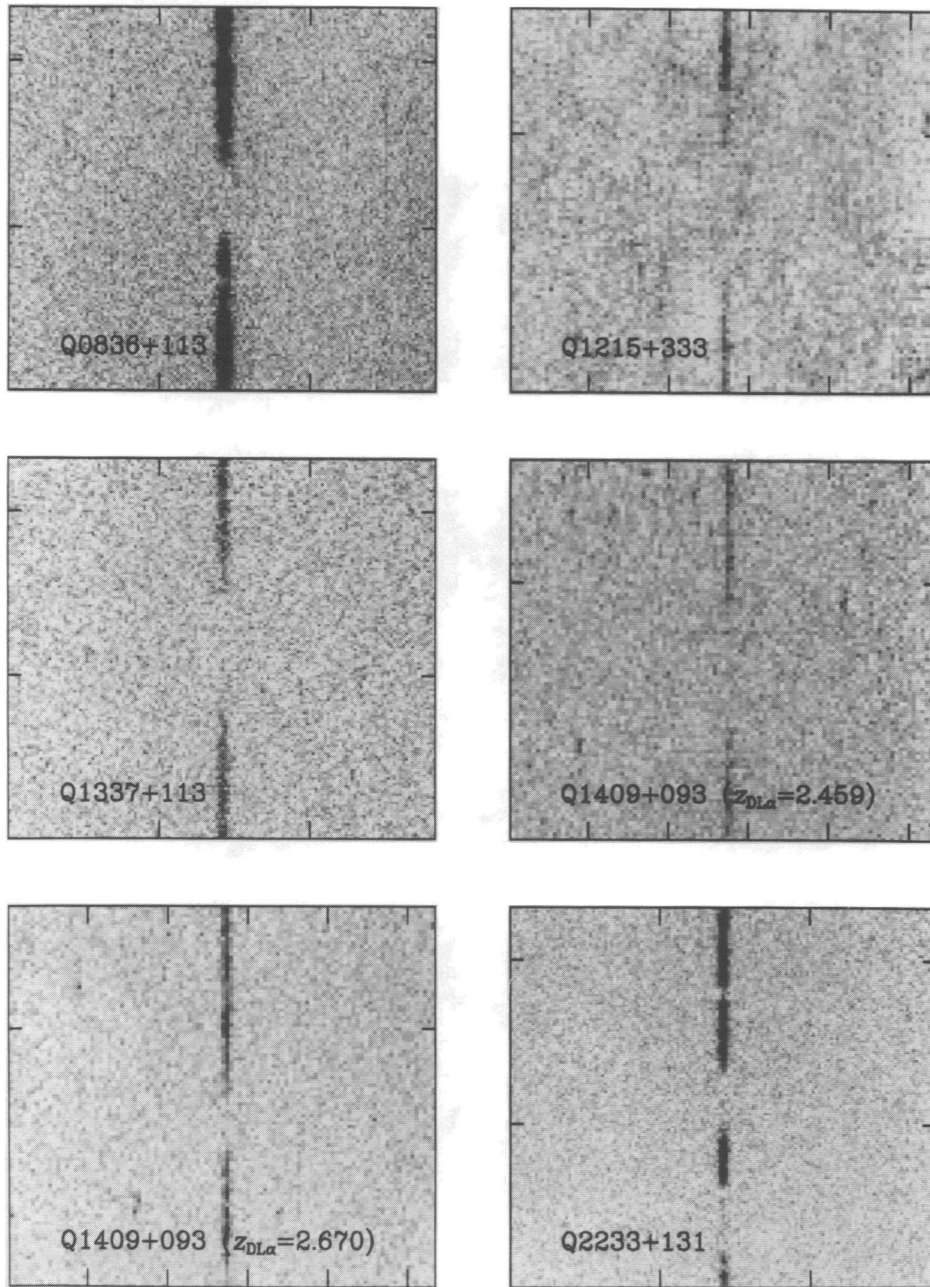
F<small>IG</small>. 1—*Continued*

Fig. 2.—Long-slit CCD spectra of six damped Lyα absorption lines toward five high-redshift QSOs. Only the region of the spectrum centered on each damped absorption line is shown. Wavelength increases from bottom to top. Tick marks represent 50 Å vertically and 30″ horizontally. No significant Lyα emission is evident in or near any of the absorption-line troughs.

The sensitivity of the final images to faint Lyα emission depends on the spectral and spatial resolutions, the integration time, the atmospheric seeing, and the system throughput at the particular wavelength region of the observation. In most cases, a source with an emission-line flux of a few $\times 10^{-17}$ ergs s^{-1} cm^{-2} would appear at approximately a 3 σ level; the exact limits on spectrally and spatially unresolved emission-line sources for each image and spectrum are presented in Table 3.

3.2. The Q0836 + 113 Field

The line of sight toward the radio-quiet QSO Q0836 + 113 ($z_{em} = 2.696$) is both complex and controversial. The spectrum

shows not only a damped Lyα system at $z = 2.467$, but also two Mg II absorbers at $z = 0.368$ and $z = 0.788$ and a C IV system at $z = 1.822$ (Turnshek et al. 1989). As noted in § 2, the damped cloud has been the object of intense scrutiny, giving rise to the divergent claims of an unresolved emission spike (HPF) and an ultrafaint extended patch of Lyα emission (Wolfe et al. 1992).

Although our Fabry-Perot on-band images of the Q0836 + 113 field showed no Lyα emission, the *off-band* C III] image, which was tuned to match the wavelength of redshifted [O II] $\lambda 3727$ for the Mg II cloud at $z = 0.788$, shows a strong, clear detection of emission 3″6 to the northeast of the QSO at
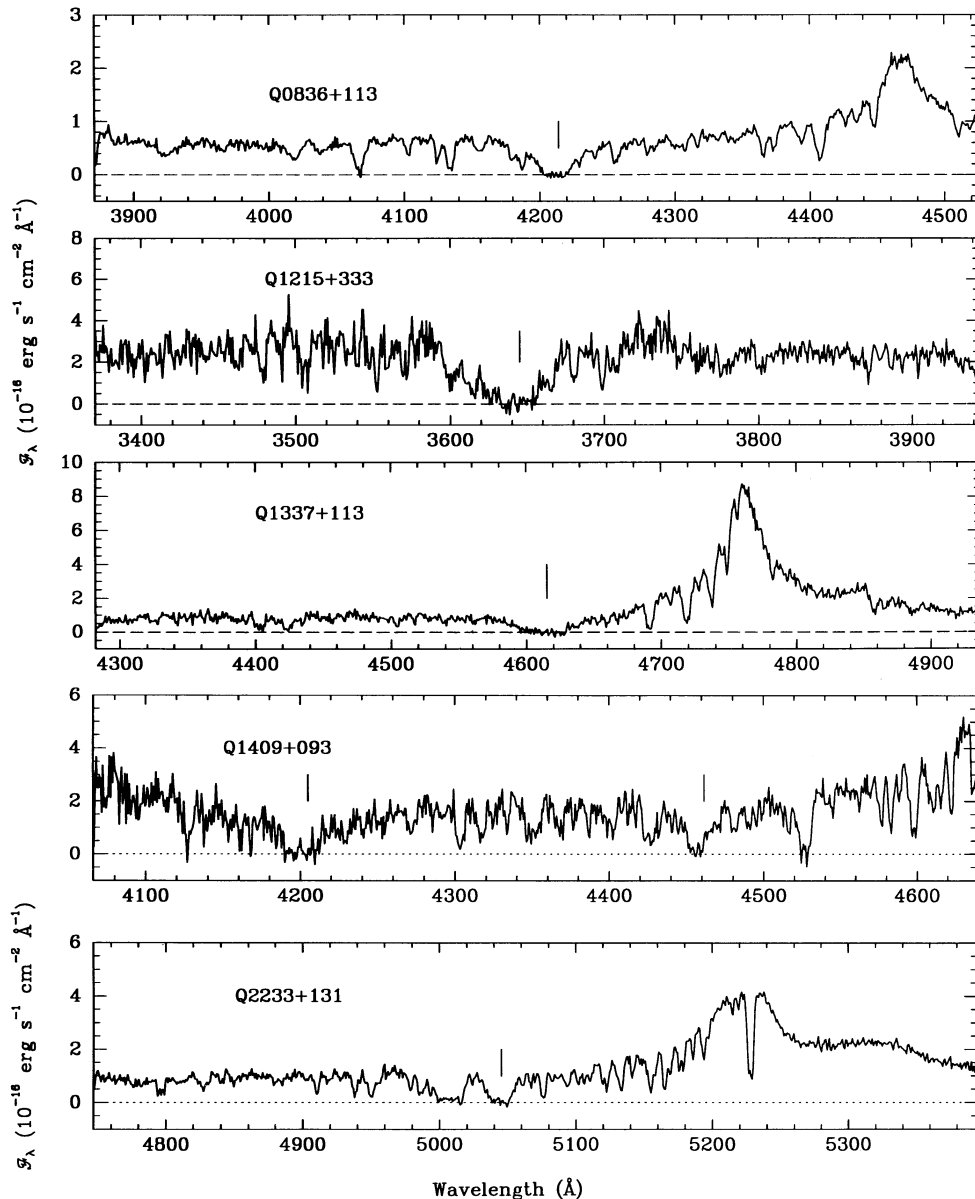
FIG. 3.—One-dimensional extracted spectra of the five QSOs shown in Fig. 2. The center of each damped Lyα absorption line is marked by a vertical line.

P.A. = 11°, while the *on-band* C III] image (= off-band for [O II] λ3727 from the $z = 0.788$ cloud) shows nothing at the same location. The total flux measured was $7 \pm 1 \times 10^{-17}$ ergs s⁻¹ cm⁻², and the patch appears marginally extended, with FWHM ~ 2″2. Both images are shown in Figure 4.

To confirm the hypothesis that the line emission observed with the FP in the C III] *off*-band frame was in fact redshifted [O II] λ3727 from the lower redshift Mg II system, we obtained long-slit spectra of the object with the Red Channel CCD Spectrograph at the MMT on 1990 March 23 (UT). Using a 270 lines mm⁻¹ grating in first order and a blocking filter to prevent second-order light from contaminating the spectrum resulted in a resolution with a 1″5 × 180″ slit of 13.5 Å over the range 3971–6815 Å. The spectral region and resolution were chosen to cover both Lyα for the damped Lyα cloud and [O II] λ3727 for the Mg II system. The slit was placed on the QSO at P.A. = 15° for the first three 1800 s integrations, a compromise

between an early estimate of the observed positions of Wolfe et al.'s object and the 6661 Å emission source; but the lack of a detection immediately visible at the telescope prompted us to change to P.A. = 10°, closer to the measured position of our source, for the remaining three exposures (as it turned out, the [O II] λ3727 emission was visible in all the individual images after data reduction). At a distance of 3″6 from the QSO, the difference of 5° corresponds to 0″3, negligible for the 1″5 slit and the 1″8 seeing, especially for an extended source. The spectrophotometric standard star G191 B2B was observed through the same slit for flux transformation. The data were reduced in the usual way and co-added to produce a single two-dimensional spectrum.

A faint but clear continuum spectrum is visible at the expected separation, 4″, from the QSO spectrum. Furthermore, a strong emission line is visible at 6661 ± 3 Å, the exact wavelength of redshifted [O II] λ3727 for the Mg II system at

TABLE 3

SUMMARY OF LIMITS ON Lyα EMISSION

FIELD	$z_{DL\alpha}$	FP/SP[a]	$F_{Ly\alpha}$[b]	$L_{Ly\alpha}$ AND SFR[c]	
				$q_0 = 0.1$	$q_0 = 0.5$
Q0045−0341......	2.810	FP	2.1	0.7	0.3
Q0201+3634......	2.461	FP	3.6	0.9	0.4
Q0336−0142......	3.061	FP	3.6	1.6	0.7
Q0836+113	2.467	FP	1.8	0.4	0.2
		SP	0.9	0.2	0.1
Q0913+0715......	2.618	FP	2.8	0.8	0.4
Q1209+0919......	2.581	FP	4.2	1.1	0.5
Q1215+333	1.998	SP	6.3	0.8	0.4
Q1337+113	2.796	FP	1.1	0.4	0.2
		SP	4.4	1.5	0.7
Q1409+093	2.459	SP	5.0	1.2	0.6
	2.670	SP	5.0	1.5	0.7
Q2233+131	3.150	SP	2.4	1.1	0.5

[a] Fabry-Perot imaging or long-slit spectroscopy.

[b] Flux limit (3 σ) in units of 10^{-17} ergs s^{-1} cm^{-2} for an unresolved pure line emission point source.

[c] Lyα luminosity limit (3 σ) in units of $10^{42} h_{100}^{-2}$ ergs s^{-1}; also, limit on star formation rate in $h_{100}^{-2} M_\odot$ yr^{-1}, assuming case B recombination with no extinction by dust.

$z = 0.788$. The continuum is visible over almost the entire spectrum (although not at the blue end, where the system throughput drops rapidly) at an average level of $1 \pm 0.3 \times 10^{-18}$ ergs s^{-1} cm^{-2} Å^{-1} at 5500 Å, corresponding to $V \sim 24.0$. At the red and blue ends of the spectrum, the object's continuum brightness is estimated at $R \sim 23.4$ and $B \sim 25.4$, but as a result of insufficient spectral coverage, the inherent errors of

slit photometry, and the low signal-to-noise ratio, these values may be in error by more than 0.5 mag. The line flux measured was $1 \pm 0.3 \times 10^{-16}$ ergs s^{-1} cm^{-2}, in good agreement with the value obtained from the FP observations; the observed equivalent width is then $W_{Obs} \sim 120$ Å, which at $z = 0.788$ corresponds to a rest equivalent width $W_0 = 67$ Å. A one-dimensional optimally extracted spectrum of the object is shown in Figure 5.

No other emission lines are visible anywhere in the two-dimensional or the extracted spectrum, although Lyα emission at 4493 Å and UV continuum from the background QSO severely contaminate the blue end. We believe that together with the perfect wavelength agreement predicted by the absorption-line redshift, this confirms the identification of the emission line as [O II] $\lambda 3727$ from the $z = 0.788$ absorber; if the emission line were Hβ at $z = 0.37$, one would expect [O II] $\lambda 3727$ at 5107 Å, or if it were [O III] $\lambda 5007$ at $z = 0.33$, one should see Hβ at 6467 Å and/or [O II] $\lambda 3727$ at 4958 Å, but none of these is seen.

The low signal-to-noise ratio near the damped Lyα line, which is mostly a result of the grating blaze, precludes this image from being used to set interesting limits on emission from the damped system, or to confirm the HPF detection.

We discuss the implications of these observations of the Mg II cloud in the following section.

4. DISCUSSION

4.1. Star Formation Rates Assuming Case B Recombination

Apart from the detection of [O II λ3727 emission from the Mg II system at $z = 0.788$ toward Q0836+113, all the obser-
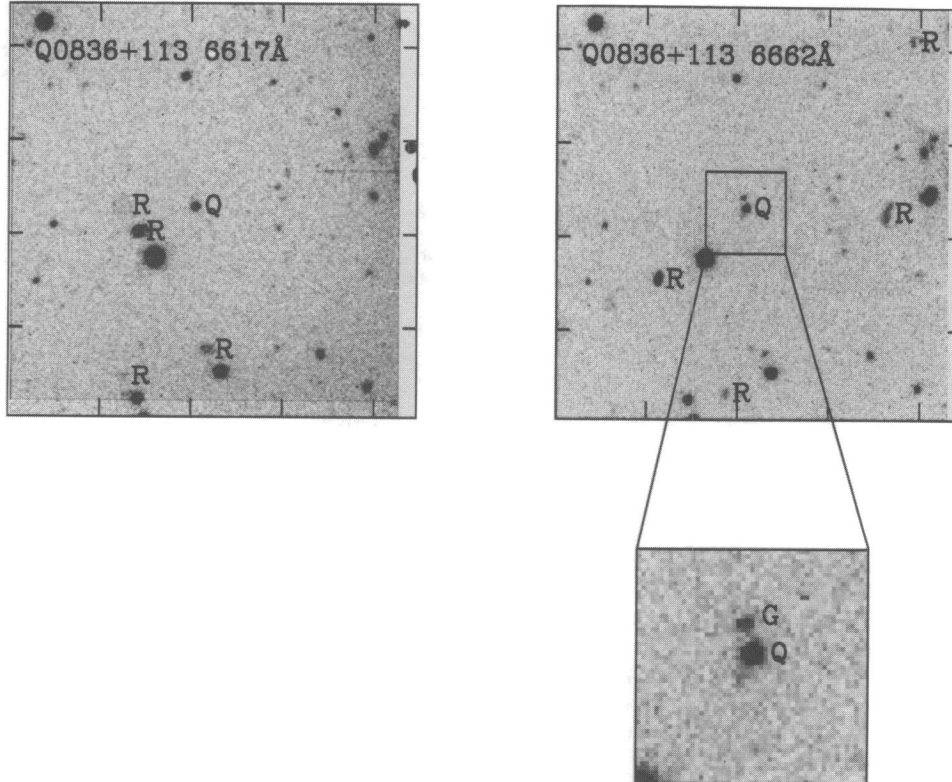

FIG. 4.—Fabry-Perot narrow-band images of the Q0836+113 field. *Left*: On-band C III] ($z = 2.467$) = off-band [O II] ($z = 0.788$). *Right*: Off-band ($z = 2.467$) = on-band [O II] ($z = 0.788$). The QSO is labeled "Q," and internal ghost reflections are labeled "R." The closeup at lower right shows the extended redshifted [O II] $\lambda 3727$ emission (labeled "G") associated with the Mg II absorber at $z = 0.788$.
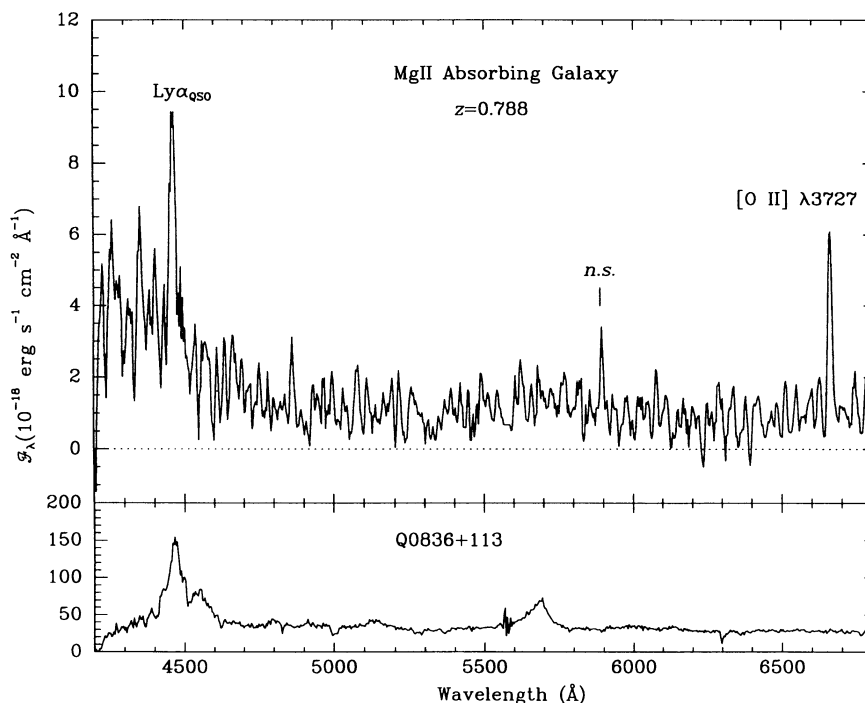
Fig. 5.—Spectrum of object "G" from Fig. 4. The emission line matching the wavelength expected for [O II] λ3727 from the Mg II absorber at $z = 0.788$ is labeled, as are a poorly subtracted night-sky line ("n.s.") and Lyα emission line and UV continuum contamination from Q0836+113, 4″ away. The lower panel shows the spectrum of the QSO, extracted from the same image.

vations reported here produced null results; we were unable to find any additional Lyα galaxies of the sort identified near the PHL 957 and Q0000−2619 damped Lyα clouds, and our target clouds themselves appear dark in Lyα down to the faintest flux limits currently practical.

We can use our limits on Lyα emission, typically $\sim 3 \times 10^{-17}$ ergs s^{-1} cm^{-2} (3 σ), to constrain the emergent flux of ionizing photons and therefore to estimate corresponding limits on star formation rates in the damped Lyα clouds. In performing this calculation, we assume negligible destruction by dust, an uncertain assumption that we will discuss further below. If we assume case B recombination in gaseous nebulae surrounding regions of star formation, then the expected ratio of Lyα to Hα flux is $F_{Ly\alpha}/F_{H\alpha} = 10$. Kennicutt (1983) parameterized the total star formation rate (SFR) of local spiral galaxies in terms of the total observed Hα luminosity as SFR ($M_\odot$ yr^{-1}) $\sim L(H\alpha)/10^{41}$ ergs s^{-1}, assuming a modified Miller-Scalo/Salpeter initial mass function; this then implies SFR $= L(Ly\alpha)/10^{42}$ ergs s^{-1}. Using standard cosmological equations to transform from observed flux to intrinsic luminosity, we therefore calculate typical star formation rates in the damped clouds of SFR ≤ 0.3–0.7 h_{100}^{-2} $M_\odot$ yr^{-1} for $q_0 = 0.5$–0.1. These results are summarized for each field in Table 3.

Typical star formation rates for the local Sc galaxies in Kennicutt's (1983) sample are ~ 10 $M_\odot$ yr^{-1}; the Milky Way probably processes a few solar masses per year of gas into stars. Our limits on star formation rates in the damped Lyα clouds therefore correspond to galaxies considerably more quiescent than normal spiral galaxies today, in stark contrast to the dramatic predictions of such early galaxy formation models as Partridge & Peebles (1967), or even more conservative models such as Baron & White (1987). Either the damped Lyα clouds do not represent young star-forming galaxies in any recognizable

form, or else the interpretation of our limits on Lyα emission is less straightforward than we have assumed above.

The conversion of Lyα flux to star formation rate depends heavily on the assumed IMF. Our interpretations of the SFRs in high-redshift galaxies are generally cast in the paradigm of local galaxies and star-forming regions, but these may be misleading assumptions. A top-heavy or a truncated IMF can produce widely varying amounts of ionizing UV flux, and metallicity also comes into play in the form of line blanketing, so the limits on Lyα emission must be taken with a grain of salt. In general, however, the various factors conspire to make the present limits conservative rather than unreasonable.

4.2. Dust in Damped Lyα Systems

Probably the largest uncertainty plaguing our analysis of limits on Lyα emission is the quantity and distribution of dust in the damped clouds. Since Lyα is a resonance line with optical depths typically exceeding 10^6, Lyα photons produced by nebulae surrounding hot stars will scatter multiply in the damped cloud's neutral hydrogen before escaping; any Lyα photon encountering a dust grain before the edge of the cloud will be absorbed. The net effect is almost certainly a decrease in the emergent Lyα flux, although the amount of decrease is highly geometry dependent; for example, hollow wind-formed chimneys in the interstellar medium (ISM) would greatly facilitate the escape of line photons. The two detections of Lyα emission in the PHL 957 and Q0000−2619 fields, as well the extended regions around high-redshift radio galaxies, clearly demonstrate the possibility for Lyα photons to escape in some situations. Neufeld (1991) pointed out that under certain multiphase geometries, Lyα emission may actually be enhanced relative to continuum radiation, although the conditions are probably not met in the damped Lyα clouds discussed here.

How much dust do the damped Lyα clouds contain, and is it enough to quench Lyα emission completely? Two techniques have been employed to answer these questions, and both seem to favor an average ratio of dust to gas on the order of 1/10 the local Galactic value. Pei, Fall, & Bechtold (1991) reported that QSOs behind known damped Lyα clouds were statistically redder than QSOs without intervening damped clouds. Assuming the reddening to be a result of dust in the damped clouds (though not Galactic-type dust, which would have produced an absorption feature that is not seen), they calculate that the dust-to-gas ratio necessary to explain the observed effect corresponds to 5%–20% of the Milky Way's value. Charlot & Fall (1991) then use these values to estimate the attenuation of Lyα photons, concluding in general that allowable levels of dust in the clouds that had been searched for Lyα emission could easily hide many tens of solar masses of star formation, assuming certain dust distributions and disk orientations.

Another approach to estimating the dust content of damped Lyα clouds consists of measuring the gas-phase metallicities or molecular abundances directly in individual clouds via absorption lines, and then drawing on our knowledge of the local ISM to infer dust properties (Meyer & Roth 1990; Meyer & York 1987; Lanzetta, Wolfe, & Turnshek 1989; Pettini, Boksenberg, & Hunstead 1990; Levshakov et al. 1989; Rauch et al. 1990; Pettini et al. 1994). Virtually all these studies have concluded that the dust content and metallicities of damped Lyα clouds are significantly lower than those in the solar neighborhood. For example, Pettini et al. (1994) and Meyer & Roth (1990) find that in the spectra of 21 damped Lyα clouds, the relative line strengths of Cr II, which is easily depleted onto dust grains, and Zn II, which is not, imply dust-to-gas ratios typically $\lesssim$10% the Milky Way value, and in one case as low as 3% the Galactic value. Furthermore, in one case (the absorber at $z = 2.076$ toward Q2206−199), examination of additional metal lines, including O I, Si II, and Si IV, yields an extremely low metallicity, [Si/H] ∼ −2.8, i.e., less than 1/100th solar (Rauch et al. 1990). Observations of two of the damped clouds studied here are consistent with low dust content: Q1215+333 (Meyer & Roth 1990) and Q1337+113 (Lanzetta et al. 1989).

Extrapolating the detailed nature of the ISM in the solar neighborhood to clouds with uncertain geometries, sizes, and physical conditions at look-back times greater than half a Hubble time is certainly risky. While measuring the gas-phase abundances of heavy elements has yielded metallicities and dust abundances consistent with the statistical reddening method, Pei et al. (1991) caution that the unknown dust composition and, perhaps, different abundance ratios from those seen in the Galaxy make the Ni-Cr-Zn measurements less dependable than they are when applied locally, and they argue that the observed gas-phase abundances are in fact compatible with somewhat higher *total* metallicities and dust levels than usually quoted. This in turn implies that Lyα emission from the damped clouds may be heavily extinguished, and that star formation rates could be very high despite the null results reported here and previously.

Certainly we should expect some clumpiness in the damped clouds, perhaps analogous to the Milky Way, where N(H) varies by over an order of magnitude (Burstein & Helies 1982) and where star formation is presumed to originate in dense molecular clouds, rather than uniformly across the entire disk. Such sites of star formation may pollute themselves quickly with metals and dust, even if the original abundances are primordal, possibly reaching 0.5 times solar metallicity by 5×10^6 yr after the onset of star formation (Lequeux et al. 1981), while mixing with other regions in the same galaxy may take place on timescales long compared to the lifetimes of massive stars (Kunth & Sargent 1986), producing an inhomogeneous ISM in the short term. While dust production is frequently thought to occur in the asymptotic giant branch of post–main-sequence stellar evolution, it is also observed to form in supernova explosions, which could have a large effect on the ISM in sites of recent massive star formation. The sight lines to background QSOs therefore may preferentially sample the thinner, less enriched medium rather than the dense clouds supporting massive star formation, possibly resulting in underestimates of the chemical abundances in the dense clouds (see Fall & Pei 1993); meanwhile, if self-enrichment with dust in these clouds progresses at a reasonable rate, then any Lyα-bright phase may last only a fraction of the lifetime of massive stars, thus escaping detection unless the absorber is observed the onset of star formation.

Local star-forming galaxies can provide us with some useful lessons. Using the *International Ultraviolet Explorer* (*IUE*) to search for Lyα emission from nearby extragalactic H II regions, radio galaxies, and blue star-forming galaxies (redshifted only enough to avoid the strong geocoronal Lyα line), Meier & Terlevich (1981), Ferland & Osterbrock (1985), Hartmann et al. (1988), Deharveng, Joubert, & Kunth (1986), and Terlevich et al. (1993) have registered detections in radio galaxies approaching the expected case B value Lyα/Hβ ∼ 30, but in general the levels for the radio-quiet objects range from 0 to $\frac{1}{10}$ the case B prediction. There appears to be a trend of weaker Lyα emission from the more metal-rich galaxies, supporting the view that dust produced in stellar processing is responsible for quenching Lyα photons; systems with metallicities around 0.1 times solar seem to allow Lyα to escape at a level down by a factor of 10 from the case B value. As Terlevich et al. (1993) point out, this will make it all but impossible to detect Lyα emission from galaxies at $z = 2$ or 3 if they resemble local luminous H II galaxies.

In summary, the interpretations of our upper limits on Lyα emission are not straightforward as a result of the uncertainties of the IMF, morphology, and abundance and distribution of dust in the damped Lyα clouds. However, if we assume an average attention of Lyα emission by a factor of 10 caused by dust—a plausible amount based on measured dust-to-gas ratios, the models of Charlot & Fall (1991), reasonable morphologies, and local H II galaxies—then our limits correspond to roughly 5–10 $M_\odot$ yr^{-1}, similar to the observed star formation rates in local late-type spiral galaxies.

4.3. *The Line of Sight to Q0836+113*

It is clear from Figures 2 and 3 that no significant emission was detected from the damped Lyα cloud toward Q0836+113. Down to what flux level is this true? A careful statistical examination of the final spectroscopic image, including pixel-to-pixel rms variation as well as simulated apertures containing several pixels, showed that for an unresolved source of emission with a profile matching the instrumental spatial and spectral point spread function (PSF), the 1 σ flux level was $3.0 \pm 1 \times 10^{-18}$ ergs s^{-1} cm^{-2}; therefore the emission-line flux of 2.9×10^{-17} ergs s^{-1} cm^{-2} reported by HPF should have appeared as a 7–10 σ feature in the middle of the absorption line. A closeup portion of the one-dimensional extracted spectrum centered on

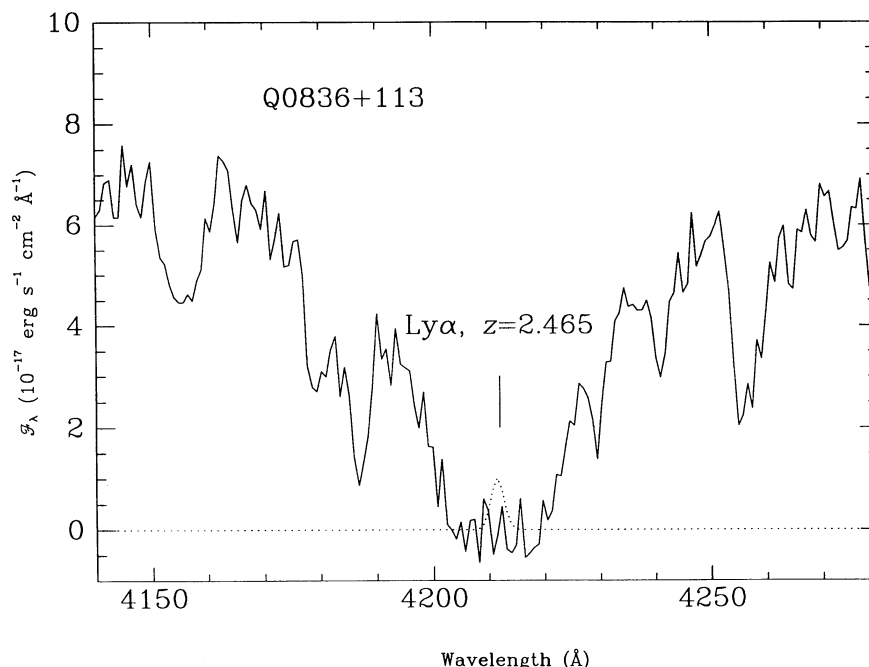FIG. 6.—Closeup of the extracted spectrum of Q0836+113 from Fig. 3, centered on the damped Lyα absorption line at $z = 2.465$. The dotted line represents a simulated emission line with total flux $F = 2.9 \times 10^{-17}$ ergs s^{-1} cm^{-2} and an FWHM matching the instrumental resolution.

the damped Lyα line is shown in Figure 6; also shown for comparison is a simulated feature matching the flux reported by HPF.

One possible explanation for the discrepancy is that HPF aligned their spectrograph slit at P.A. = 140–160°, rotating it once during each night to keep within ~10° of the parallactic angle, while we aligned ours at P.A. = 15° to coincide with the extended flux reported by Wolfe et al. (1992) and the Mg II absorbing galaxy seen in our narrow-band images. If there were an emission source not centered on the QSO line of sight but rather offset by 1″ or 2″ at P.A. ~ 150°, then some flux might have fallen down HPF's slit and still been counted in the 2″.2 bin centered on the QSO, while somewhat less flux would have been collected by our slit at its different position angle. However, both spectra were obtained in seeing of 1″.2–2″.1 with slit widths of 1″.2–1″.5, so even if the slits were placed at right angles to each other rather than an average angle of 45°, there would have been nearly complete overlap in the 1″ or 2″ region centered on the QSO. If the Lyα emission were caused by an object any farther than that from the QSO line of sight, we should have detected it in our Fabry-Perot images.

Another possible explanation for our not confirming HPF's emission is an unfortunate combination of the inherent uncertainties in the absolute flux calibrations of both their narrow-slit spectrophotometry and ours. However, even if we allow for the reported flux of 2.9×10^{-17} ergs s^{-1} cm^{-2} to be fainter by the quoted error of 30% and for our limits to be less sensitive than the nominal value by a similar amount, we still expect to have detected the emission at about the 5 σ level.

The extended Lyα flux claimed by Wolfe et al. (1991) is much fainter than that reported by HPF. We can examine the possibility that the Wolfe et al. flux could have been detected in our deep spectrum as follows. First let us assume that at the resolution of the 1991 January MMT data, 2.6 Å FWHM ≈ 200 km s^{-1} at 4214 Å, any Lyα emission line would be at most marginally resolved; this assumption is supported

by the observed widths of the metal absorption lines associated with the damped Lyα systems. Then, assuming that approximately half the total emission region would be covered by the 1″.5 slit, we can model the expected appearance of the source; the total flux falling on the slit would be $F \approx 1.4 \times 10^{-17}$ ergs s^{-1} cm^{-2} distributed roughly in a Gaussian of FWHM 6″. Such a flux level would appear at only the 2.4 σ level even if it were spatially compact. Several simulated features with these parameters were placed at random positions near the damped Lyα line in the two-dimensional spectrum of Q0836; although all were detectable by blinking between the simulated and original frames, none of them would be distinguishable a priori from noise fluctuations. Thus, these data are insufficiently sensitive to confirm Wolfe et al.'s observations directly.

Is it possible that continuum emission from the foreground Mg II system is responsible for the flux seen in Wolfe et al.'s narrow-band images? The continuum flux we detected from the Mg II galaxy was around 1×10^{-18} ergs s^{-1} cm^{-2} Å^{-1} at 5500 Å and probably varies by no more than 25% from that level at 4200 Å. Although there is no direct evidence that the galaxy is extended in emission, it certainly contains an extended envelope of some sort; the 4″ separation from the QSO line of sight corresponds at $z = 0.788$ to 16.4 h^{-1} kpc. The Mg II galaxy is thus entirely consistent with the findings of Bergeron & Boissé (1991) and Yanny et al. (1990), including its continuum and [O II] $\lambda 3727$ emission as well as its minimum size.

The total flux detected by Wolfe et al. (1991) near the position of the Mg II galaxy in their 25 Å narrow-band filter was $F = 3.9 \pm 0.5 \times 10^{-17}$ ergs s^{-1} cm^{-2} over an area approximately 3″ × 6″, giving an average monochromatic surface brightness $S = 9 \times 10^{-20}$ egs s^{-1} cm^{-2} arcsec^{-2} Å^{-1}; they attribute ~25% of this to the "starlike" object C, which they identify as the Mg II system, and ~75% to the extended object W, supposedly the damped system. If in fact all the flux were caused by continuum from the Mg II absorber at the level we

measure in our spectrum, then it would need to be spread out over a patch of sky only $3'' \times 4''$ to match the average surface brightness reported by Wolfe et al. We believe this is plausible.

The strongest argument *against* interpreting Wolfe et al.'s flux as continuum for the Mg II galaxy may be that they report no extended continuum in their deep broadband images of the Q0836+113 field, but only a pointlike feature, which they assign to the foreground system; if they reached the continuum level of the spatially extended Mg II galaxies with their narrow-band images, they should also have reached it with their broadband observations at about the 4σ level. Nevertheless, the position centroids relative to the QSO of Wolfe et al.'s object W and the [O II] $\lambda 3727$ emission seen in the FP images agree to $0''.2$. The coincidental superposition of *two* emission regions from entirely unrelated absorbing galaxies along the same line of sight is improbable—about a 2% chance that two 1 arcsec^2 sources will be randomly superposed within a $4''$ radius circle. As mentioned above, the underlying Mg II galaxy is certainly extended on a scale of several arcseconds, so we can imagine that any emission might fall off gradually with distance from regions of intense star formation activity. While there is some discrepancy in the flux values observed versus those expected in this scenario, all the detections are at low signal-to-noise ratio and are probably pushing the limits of the accuracy of the data. However, we must conclude that we cannot rule out the identification of Wolfe et al.'s detection as Lyα.

Finally, Wolfe et al. (1992) point out an additional feature in their narrow-band images, $6''$ to the southwest of the QSO line of sight, with an enhanced flux compared to the broadband measurement; perhaps *this* is in fact the damped system! The object is too faint to appear in our Fabry-Perot frames, but a Lyα line could show up in a deep low-resolution spectrum.

5. SUMMARY

We have presented new Fabry-Perot Lyα images of seven high-redshift QSO damped Lyα clouds and two-dimensional spectra of six. We have found no convincing evidence for Lyα emission in any of the fields. We were unable to confirm the unresolved Lyα emission in the damped Lyα absorption trough at $z = 2.467$ toward Q0836+113 reported by HPF. Furthermore, we propose that the extended emission reported by Wolfe et al. (1992) may be continuum emission from the Mg II cloud at $z = 0.788$ toward that QSO, rather than Lyα emission from the damped cloud, although we are unable directly to confirm or rule out Lyα emission. To do that a long-slit spectrum a factor of at least 2 deeper than ours, which required two full nights at the MMT, will be necessary.

Taken at face value, our limits imply that the damped clouds are quiescent, forming at most $\sim 1 \ M_\odot \ \text{yr}^{-1}$ in the regions studied. However, observationally all allowed quantities of dust in the clouds might completely extinguish sizable Lyα fluxes, so that in fact our nondetections cannot be used to place stringent limits on the star formation rates therein. It seems likely that searching in the near-IR for redshifted optical continuum and emission lines will be a more promising technique for identifying and studying damped Lyα clouds at high redshift.

REFERENCES

Baron, E., & White, S. D. M. 1987, ApJ, 322, 585
Bergeron, J., & Boissé, P. 1991, A&A, 243, 344
Briggs, F. H. 1993, private communication
Briggs, F. H., Wolfe, A. M., Liszt, H. S., Davis, M. M., & Turner, K. L. 1989, ApJ, 341, 650
Broadhurst, T. J., Ellis, R. S., & Shanks, T. 1988, MNRAS, 235, 827
Brown, R. L., & Vanden Bout, P. A. 1991, AJ, 102, 1956
———. 1993, ApJ, 412, 21
Burnstein, D., & Heiles, C. 1982, AJ, 87, 1165
Caulet, A., & McCaughrean, M. 1992, in The Evolution of Galaxies and Their Environment, ed. D. Hollenbach, H. Thronson, & J. M. Shull (NASA Conf. Pub. 3190), 359
Caulet, A., Woodgate, B. E., Brown, L. W., Gull, T. R., Hintzen, P., Lowenthal, J. D., Oliversen, R. J., & Ziegler, M. M. 1992, ApJ, 388, 301
Charlot, S., & Fall, S. M. 1991, ApJ, 378, 471
Cowie, L. L. 1988, in The Post-Recombination Universe, ed. N. Kaiser & A. N. Lasenby (Dordrecht: Kluwer), 1
Deharveng, J. M., Buat, V., & Bowyer, S. 1990, A&A, 236, 351
Deharveng, J. M., Joubert, M., & Kunth, D. 1986, in Star-Forming Dwarf Galaxies and related Objects, ed. D. Kunth, T. X. Thuan, & J. T. T. Van (Gif-sur-Yvette: Editions Frontieres), 431
Elston, R. J., Bechtold, J., Lowenthal, J. D., & Rieke, M. 1991, ApJ, 373, L39
Fall, S. M., & Pei, Y. C. 1993, ApJ, 402, 479
Ferland, G. J., & Osterbrock, D. E. 1985, ApJ, 289, 105
Foltz, C. B., Chaffee, F. H., & Weymann, R. J. 1986, AJ, 92, 247
Francis, P. F., Woodgate, B. E., Warren, S. J., Moller, P., Mazzolini, M., Bunker, A. J., Lowenthal, J. D., & Williams, T. 1995, ApJ, submitted
Giavalisco, M., Steidel, C. C., & Szalay, A. S. 1994, ApJ, 425, L5
Hartmann, L. W., Huchra, J. P., Geller, M. J., O'Brien, P., & Wilson, R. 1988, ApJ, 326, 101
Hu, E. M., Songalia, A., Cowie, L. L., & Hodapp, K.-W. 1993, ApJ, 419, L13
Hunstead, R. W., Pettini, M., & Fletcher, A. B. 1990, ApJ, 356, 23 (HPF)
Kennicutt, R. C. 1983, ApJ, 272, 54
Kunth, D., & Sargent, W. L. W. 1986, 300, 496
Lanzetta, K. M., Wolfe, A. M., & Turnshek, D. A. 1989, ApJ, 344, 277

Lanzetta, K. M., Wolfe, A. M., Turnshek, D. A., Lu, L., McMahon, R. G., & Hazard, C. 1991, ApJS, 77, 1
Lequeux, J., Mauchera-Joubert, M., Deharveng, J. M., & Kunth, D. 1981, A&A, 103, 305
Levshakov, S. A., Foltz, C. B., Chaffee, F. H., & Black, J. H. 1989, AJ, 98, 6
Lilly, S. J., Cowie, L. L., & Gardner, J. 1991, ApJ, 369, L79
Lowenthal, J. D. 1991, Ph.D. thesis, Univ. Arizona
Lowenthal, J. D., Hogan, C. J., Green, R. F., Caulet, A., Woodgate, B. E., Brown, L., & Foltz, C. B. 1991, ApJ, 377, L73
Lowenthal, J. D., Hogan, C. J., Leach, R. W., Schmidt, G. D., & Foltz, C. B. 1990, ApJ, 357, 3
Lu, L., & Wolfe, A. M. 1994, AJ, 108, 44
Macchetto, F., Lipari, S., Giavalisco, M., Turnshek, D. A., & Sparks, W. B. 1993, ApJ, 404, 511
Meier, D. L., & Terlevich, R. 1981, ApJ, 246, L109
Meyer, D. M., & Roth, K. C. 1990, ApJ, 363, 57
Meyer, D. M., & York, D. G. 1987, ApJ, 319, L45
Moller, P., & Warren, S. J. 1993, A&A, 270, 43
Neufeld, D. A. 1991, ApJ, 370, L85
Partridge, R. B., & Peebles, P. J. E. 1967, ApJ, 147, 868
Pei, Y. C., Fall, S. M., & Bechtold, J. 1991, ApJ, 378, 6
Pettini, M., Boksenberg, A., & Hunstead, R. W. 1990, ApJ, 348, 48
Pettini, M., Smith, L. J., Hunstead, R. W., & King, D. L. 1994, ApJ, 426, 79
Pritchett, C., & Hartwick, F. 1990, ApJ, 355, L11
Rauch, M., Carswell, R. F., Robertson, J. G., Shaver, P. A., & Webb, J. K. 1990, MNRAS, 242, 698
Rhee, G. F., Loken, C., & Le Febre, O. 1993, ApJ, 406, 26
Smith, H. E., Cohen, R. D., Burns, J. E., Moore, D. J., & Uchida, B. A. 1989, ApJ, 347, 87
Solomon, P. M., Radford, S. J. E., & Downes, D. 1992, Nature, 356, 318
Steidel, C. C., & Dickinson, M. 1992, ApJ, 384, 81
Steidel, C. C., & Hamilton, D. 1992, AJ, 104, 941
Taramopoulos, A., Briggs, F. H., & Turnshek, D. A. 1994, AJ, 107, 1937
Terlevich, E., Diaz, A. I., Terlevich, R., & Vargas, M. L. G. 1993, MNRAS, 260, 3

Thomson, S. J., Djorgovski, S., & Trauger, J. 1993, in The Evolution of Galaxies and Their Environment, ed. D. Hollenbach, H. Thronson, & J. M. Shull (NASA Conf. Publ. 3190), 23

Turnshek, D. A., Macchetto, F., Bencke, M. V., Hazard, C., Sparks, W. B., & McMahon, R. G. 1991, ApJ, 382, 26

Turnshek, D. A., Wolfe, A. M., Lanzetta, K. M., Briggs, F. H., Cohen, R. D., Foltz, C. B., Smith, H. E., & Wilkes, B. J. 1989, ApJ, 344, 567

Tyson, J. A. 1988, AJ, 96, 1

Uson, J. M., Bagri, D. S., & Cornwell, T. J. 1991, Phys. Rev. Lett., 67, 3328

Wiklind, T., & Combes, F. 1994, A&A, 288, L41

Wolfe, A. M. 1993, ApJ, 402, 411

Wolfe, A. M., Turnshek, D. A., Lanzetta, K. M., & Oke, J. B. 1992, ApJ, 385, 151

Wolfe, A. M., Turnshek, D. A., Smith, H. E., & Cohen, R. E. 1986, ApJS, 61, 249

Yanny, B., York, D. G., & Williams, T. B. 1990, ApJ, 351, 377